IEEE Access
Multidisciplinary : Rapid Review : Open Access Journal

Received December 18, 2020, accepted January 2, 2021, date of publication January 8, 2021, date of current version January 15, 2021.

Digital Object Identifier 10.1109/ACCESS.2021.3050240

Visual Experimental Study on Two Phase Flow Patterns of the Evaporative Cooling System

YITAO SHI[1,2], RUI CAO[1], AND LIN RUAN[1,2]
[1]Institute of Electrical Engineering, Chinese Academy of Sciences, Beijing 100089, China
[2]School of Electronic Electrical and Communication Engineering, University of Chinese Academy of Sciences, Beijing 101400, China

Corresponding author: Lin Ruan (rosaline@mail.iee.ac.cn)

This work was supported by the National Natural Science Foundation of China under Grant 51777201.

ABSTRACT The flow pattern is of great significance for calculating boiling heat transfer and two phase flow pressure drop, and there is no uniform flow pattern diagram for the evaporative cooling system. This paper has carried out experimental research on the flow pattern in the liquid box of the surface-mounted evaporative cooling system and establish a mathematical prediction model of flow pattern transition. The experimental results show that the flow patterns are mainly bubble flow, churn flow, and misty flow in the liquid box of the surface-mounted evaporative cooling system under different thermal loads. By comparing observed flow patterns with existing flow pattern diagrams, it can be found that the existing flow pattern diagrams are not suitable for the flow pattern division of surface-mounted evaporative cooling system. A new flow pattern diagram is proposed based on the change of interfacial area concentration in the liquid box. The prediction results of the new flow pattern diagram are in good agreement with the experimental data, which provides valuable insights into the flow pattern and paves the way for further boiling heat transfer calculation of surface-mounted evaporative cooling system.

INDEX TERMS Evaporative cooling, flow pattern, visualization, transition correlation.

I. INTRODUCTION

With the continuous advancement of electronic technology, the heat flux of electronic equipment has exceeded 100w/cm^2, and the heat dissipation problem has become a bottleneck for its further development [1]. The evaporative cooling system has better than water cooling, air cooling, and other traditional cooling methods in cooling performance with the advantages of high efficiency, low power consumption, insulation, and long service life, etc. It has been successfully applied to supercomputers, IGBT converter valves, wind power generators, high-speed rail, and other equipment [2]–[5]. However, due to boiling heat transfer complexity, no accurate prediction model for high power density two phase flow heat transfer and pressure drop has been established. The flow pattern is a crucial factor affecting the boiling heat transfer. Precise flow pattern division is essential to the calculation of boiling heat transfer [6]. Therefore, the two-phase flow patterns of flow boiling should be investigated.

The associate editor coordinating the review of this manuscript and approving it for publication was Lei Wang.

There are many studies on two-phase flow patterns and the corresponding flow pattern diagrams. In the earlier research, Baker, Hewitt, and Roberts, Gould *et al.*, Taitel, and Dukler have proposed different flow pattern diagrams with the air-water system [7]–[10]. However, most of these studies did not consider the effects of fluid properties and heat transfer on the two-phase flow. Kenning *et al.* observed the flow pattern of saturated flow boiling in a narrow channel with a high-speed camera and obtained pressure and heat transfer characteristics of different flow patterns [11]. Guo established a horizontal two-phase flow experimental table according to the evaporative cooling turbine generator stator hollow conductor's structure and obtained a flow pattern transition correlation [12]. Yu Zhu *et al.* got a flow pattern that used R32 as the coolant in horizontal microchannels and studied the effects of pipe diameter, heat flow, and pressure on different flow patterns [13]. Kharangate *et al.* conducted a comprehensive analysis of the flow boiling used FC72 as the coolant in a rectangular channel, obtained a flow pattern in a rectangular channel with single-sided and double-sided heating [14]. Mosyak *et al.* experimented with air-water and steam-water flow in parallel triangular microchannels.

Different flow patterns were observed simultaneously, and developed a practical modeling approach for two-phase in microchannel [15].

Finning can strengthen the boiling heat transfer process in the channel, and it will have a particular effect on the two-phase flow pattern. To further know the mechanism of heat transfer enhancement, Many scholars have studied the impact of the two-phase flow pattern in the ribbed channel tube. Carey *et al.* studied the boiling flow pattern in the vertical rectangular channel with offset strip fins and found that no nucleate boiling is present when the flow is in the film-flow regime virtually [16]. Colombo *et al.* conducted a flow boiling and convective condensation experiment with R134a and analyzed how fin affects the flow pattern transition [17]. Yang *et al.* presented an improved flow pattern map for flow boiling in horizontal micro-fin tubes [18].

Many researchers have already studied two-phase flow patterns, flow pattern transition, and most flow pattern diagrams developed for specific experimental conditions. The conclusion obtained is not enough to reveal the mechanism of flow pattern transition. Besides, an investigation on the liquid box of the evaporative cooling system is rarely reported, and the flow pattern transition mechanism is still lacking, so it is necessary to study the two phase flow pattern in the liquid box of the evaporative cooling system. This paper experimented on flow characteristics under several operating conditions covering thermal loads from 100W to 800W and captured the flow patterns. The experimental results show that the flow patterns in the liquid box are mainly bubble flow, churn flow, and misty flow under different thermal loads. There is no slug flow in the liquid box, which is a significant difference from traditional studies. The transition mechanism is studied by analyzing the effect of relevant parameters on two-phase flow pattern transitions. Moreover, the change of interfacial area concentration at the liquid box outlet is used as a quantitative criterion for the flow pattern transition based on the flow and heat transfer mechanism, and a prediction model is established for a new flow pattern map. The results provide an essential theoretical basis for evaporative cooling technology in the cooling of electronic equipment.

II. EXPERIMENTAL SYSTEM

The surface-mounted evaporative cooling system is shown in figure 1, which consists of four parts: the liquid box, the condenser, the liquid pipe, and the vapor-liquid pipe. The coolant is heated to the vapor phase in the liquid box and then flows up to the condenser through the vapor-liquid pipe under buoyance force. In the condenser, the vapor condenses to a liquid and flows back to the liquid box through the liquid pipe under the gravity force. The liquid box (230 mm × 230 mm × 20 mm) consists of a liquid box and a heating block, which simulates the heat dissipation of an electronic chip. The transparent inspection window is attached to the front of the liquid box through which the flow patterns can be captured. The heating block is closely tied to the liquid box, and thermal grease is applied between the two to reduce the contact thermal resistance. The large surface area of the liquid box can fully cover the heating block to achieve the rapid and efficient cooling of the heating block. A detailed description of the experimental system can be found in reference [5].

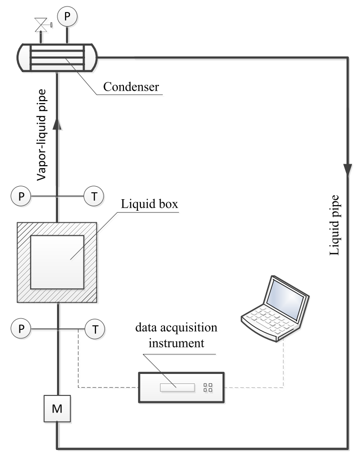

FIGURE 1. Experimental system diagram.

System measuring instruments mainly include T-type thermocouples, pressure sensors, flow meters, etc. To avoid the uneven flow field at the inlet and outlet of the liquid box to affect the measurement accuracy, we arrange the flowmeter 15cm below the liquid box inlet. All measurement data are transmitted to the computer through the Fluke 2860A data acquisition instrument. The main parameters of the instruments are reported in Table 1.

TABLE 1. Measurement instruments.

Name	Range	Uncertainty
Pressure sensor	0~50kpa	±0.05%
Thermocouple	-100 ~+600°C	±0.2 °C
Flow meter	5~1000ml/min	±0.5%

Before the experimental setup running, the non-condensable gas in the system is discharged through the exhaust valve of the condenser, and then the experiment is started. The thermal load gradually increased from 100w to 800w with intervals of 50W. The system reaches a steady condition when the temperature changes less than 0.5°C and start recording relevant experimental data.

III. SIMPLIFIED CALCULATION

Researchers have established many prediction models for flow pattern transition from the perspective of the two phase flow mechanism. Taitel *et al.* established a more comprehensive application prediction model based on a two-phase flow transition mechanism, which fully considers the effects of fluid physical properties and flow channel size [19]. Ishii *et al.* established three-dimensional and one-dimensional two-fluid two-phase flow models based on the conservation of momentum and energy. The model introduced a new two-phase interface mass, momentum, and energy exchange relationship [20]. Mishima *et al.* used void fraction as a judgment parameter to establish a prediction model for the flow pattern transition of circular and rectangular channels [21]. Chen carried out a detailed analysis of the effect of small channel size on flow pattern transition and established different flow pattern transition models based on more than 2000 experimental data [22]; Lu *et al.* established a prediction model of flow pattern transition based on the characteristics of the interface transfer mechanism of two-phase flow. The study found that the extreme point of the interfacial area concentration on the relationship curve was the transition from bubble flow to slug flow and widely used in unstable or transient conditions [23]. These mechanism models reveal the flow pattern transition process more comprehensively. However, these prediction models are mostly based on the specific circulation system and do not suitable for self-circulation systems. Therefore, it is necessary to establish a liquid box calculation model applicable to the surface mounted evaporative cooling system.

In this paper, the boiling two phase flow process of the coolant in the liquid box changes only along the axial direction by ignoring the horizontal difference in the liquid box channel according to the lumped parameter method. The coolant undergoes two liquid-specific heat absorption processes and vapor-liquid boiling heat transfer in turn in the liquid box, as shown in Figure 2.

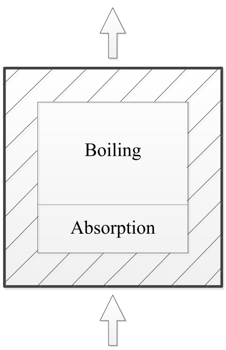

FIGURE 2. Liquid box physical model.

A. EQUATIONS

The flow pattern change in the liquid box occurs in the vapor-liquid boiling heat transfer section. Therefore, the energy, momentum, mass, and interface conservation equations are established for the vapor-liquid boiling heat transfer section, as shown below.

Heat absorbed by coolant:

$$q_d = \frac{U^2}{R} - q_s \tag{1}$$

Continuity equation:

$$\frac{\partial(\alpha\rho_g u_g)}{\partial z} = \Gamma_g \tag{2}$$

$$\frac{\partial((1-\alpha)\rho_l u_l)}{\partial z} = \Gamma_l \tag{3}$$

Energy equation:

$$dQ = \frac{\partial \rho u h}{\partial z} \tag{4}$$

Momentum equation:

$$\frac{\partial(\alpha\rho_g u_g^2)}{\partial z} = -\alpha\frac{\partial p}{\partial z} + F_{gw} - \alpha\rho_g g + \Gamma_g u_i + F_{gl} \tag{5}$$

$$\frac{\partial((1-\alpha)\rho_l u_l^2)}{\partial z} = -(1-\alpha)\frac{\partial p}{\partial z} + F_{lw} - (1-\alpha)\rho_l g + \Gamma_l u_i + F_{\mathrm{lg}} \tag{6}$$

Interface conservation equation:

$$\Gamma_g = \Gamma_l \tag{7}$$

$$F_{gl} = -F_{\mathrm{lg}} \tag{8}$$

Add equation (5) and (6) to get:

$$\frac{\partial p}{\partial z} = F_{lw} + F_{gw} - (\alpha\rho_g + (1-\alpha)\rho_l)g - \frac{\partial(\alpha\rho_g u_g^2)}{\partial z} - \frac{\partial((1-\alpha)\rho_l u_l^2)}{\partial z} \tag{9}$$

Substitute equation (9) into equation (6) to get:

$$F_{gl} = \alpha F_{lw} - (1-\alpha)F_{gw} - \Gamma_g u_i + (1-\alpha)\frac{\partial(\alpha\rho_g u_g^2)}{\partial z} - \frac{\partial((1-\alpha)\rho_l u_l^2)}{\partial z} - \alpha(1-\alpha)(\rho_l - \rho_g)g \tag{10}$$

where q_d, and q_s are effective thermal load and loss thermal load; U is loading voltage; R is the resistance of heating block; α is Void fraction; ρ is density; u is velocity; Γ is the mass source; p is pressure; F is friction force, subscripts w, l, and g are wall, liquid, and vapor.

B. EMPIRICAL CORRELATION

Equation (10) contains three unknown variables: wall friction, vapor-liquid drag, and void fraction. The drag force of the vapor-liquid section adopts the empirical correlation formula proposed by Miropolskii *et al.* [24], and the slip ratio adopts the calculation correction offered by Ishii and Mishima *et al.* [20], and detailed calculation methods are as follows:

Wall friction:

$$F_{kw} = -\frac{1}{8}A_{kw}u_k^2 f_{kw} \quad (\mathrm{k = g, l}) \tag{11}$$

Among:

$$f_{kw} = 64\mathrm{Re}_k^{-1} \quad (\mathrm{Re} < 2300) \tag{12}$$

$$f_{kw} = 0.3164\mathrm{Re}_k^{-0.25} \quad (\mathrm{Re} > 2300) \tag{13}$$

Wall Reynolds number:

$$\mathrm{Re}_k = \frac{D u_k \rho_k}{\mu_k} \tag{14}$$

Interface drag:

$$F_{gl} = -\frac{1}{8}C_D A_i \rho_l \left|u_r\right| u_r \tag{15}$$

Bubble Reynolds number:

$$\mathrm{Re}_b = \frac{D_b u_b \rho_l}{\mu_l} \tag{16}$$

Bubble diameter:

$$D_b = D_{b0}(\alpha < 0.1) \tag{17}$$

$$D_b = D_{b0}(\frac{9\alpha}{1-\alpha})^{\frac{1}{3}} \quad (\alpha \geq 0.1) \tag{18}$$

Void fraction:

$$\alpha = \frac{1}{1 + S\frac{\rho_g}{\rho_l}\frac{1-x}{x}} \tag{19}$$

Slip ratio:

$$S = 1 + \frac{13.5}{Fr^{5/12}\mathrm{Re}_l^{1/6}}(1 - \frac{p}{p_{cr}}) \tag{20}$$

where A is flow area; f is friction factor; x is vapor quality; Fr is Froude number; p is pressure; subscripts cr is a critical state.

IV. RESULTS AND DISCUSSION

In this section, the flow pattern diagrams of the liquid box under different thermal loads are preliminarily divided by analyzing the relevant influencing factors based on experimental images. Then the experimental data of the flow pattern is compared with the existing flow pattern maps. Finally, we propose a new flow pattern diagram for the surface-mounted evaporative cooling system.

A. FLOW PATTERN VISUALIZATION

Figures 3-5 appear three flow patterns of bubble flow, churn flow, and mist flow in the liquid box during the thermal load increase. As shown in Figure 3, bubbles are generated in only some areas, and the flow pattern is the bubble flow when the back temperature of the liquid box is low in the early stage of low thermal loads. As the thermal load rises, the generation of the bubbles increases to fill the liquid box in Figure 4. The flow pattern changes from bubble flow to churn flow when the average coolant temperature tends to the saturation temperature in the liquid box. When the thermal load is close to the critical heat flux of the system, the mist flow begins to appear at the outlet of the liquid box in Figure 5, which indicates that the heat transfer in the liquid box starts to deteriorate due to insufficient circulation power. These are significantly different from the traditional circular or rectangular channel flow patterns. The large cross-section ratio of the liquid box and rib disturbance restricts the coalescence of bubbles to form large bubbles, causing the transition from churn flow to mist flow.

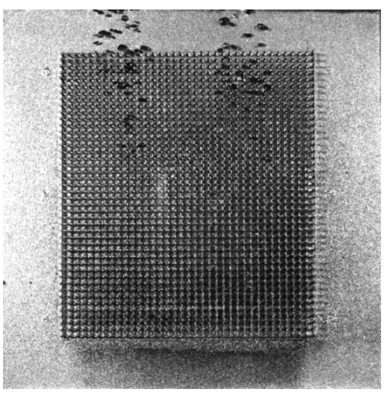

FIGURE 3. Bubble flow boiling.

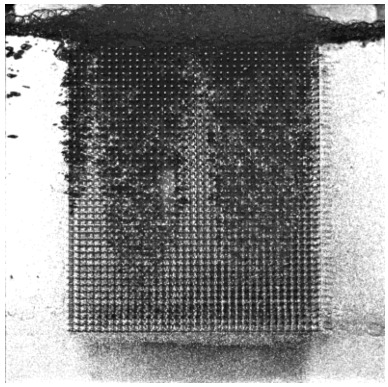

FIGURE 4. Churn flow boiling.

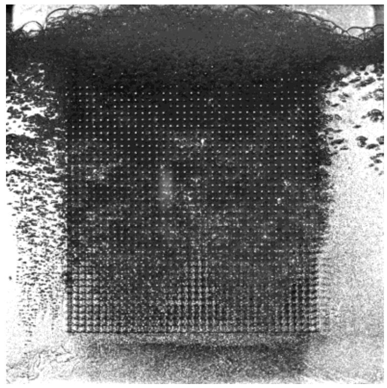

FIGURE 5. Mist flow boiling.

With the increase of thermal load, the flow pattern change reflects the change of heat transfer mode in the liquid box. When the flow pattern is in the bubble flow, the enhanced heat transfer caused by the bubbles disturbance is limited due to the small amount of bubble generation. Therefore, convection heat transfer is the primary heat transfer mode in the liquid box. When the flow pattern is changed to saturated bubble boiling, bubble generation and disturbance become the primary heat transfer mode in the liquid box. The boiling heat transfer in the liquid box is rapidly improved, as shown in Figure 6. As the thermal load approaches the maximum value, the mist flow pattern appears in the liquid box. At this time, the heat transfer mode begins to change to vapor cooling, which means that the heat transfer coefficient decreases rapidly, and the temperature on the back of the liquid box begins to rise rapidly.

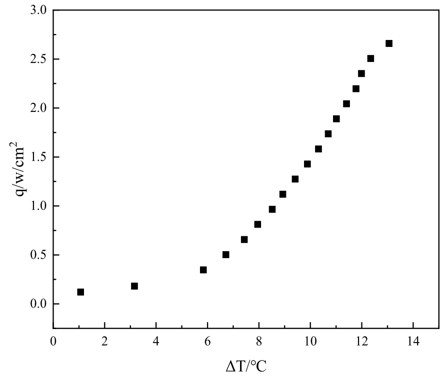

FIGURE 6. Boiling curve.

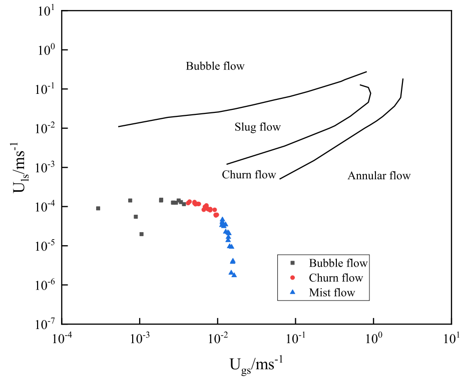

FIGURE 8. Comparison of experimental data and chen flow pattern diagram.

B. FLOW PATTERN DIAGRAM

Figures 7−9 show the comparison between the experimental data and existing flow pattern. The Mishima flow pattern map can cover the bubble flow in Figure 7. However, the flow pattern diagram does not predict churn flow and mist flow. The Chen flow pattern map is in poor agreement with the experimental data. The main reason is that this model considers the influence of the channel size on the flow pattern, which is more suitable for the flow pattern division of the microchannel. Figure 9 shows that the Lu flow pattern diagram can predict bubble flow, but a small number of experimental results of churn flow are consistent with the predicted values. Neither figure 7−9 can accurately predict the mist flow in the evaporative cooling system.

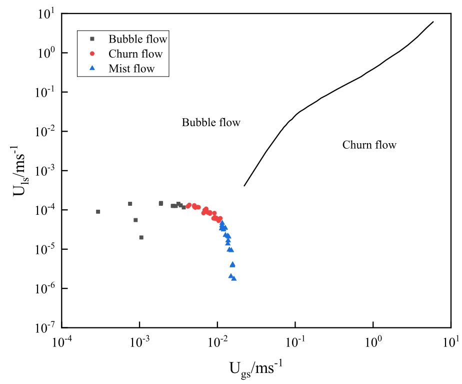

FIGURE 9. Comparison of experimental data and lu flow pattern diagram.

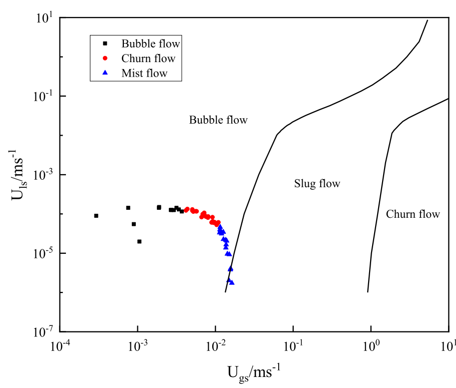

FIGURE 7. Comparison of experimental data and mishima flow pattern diagram.

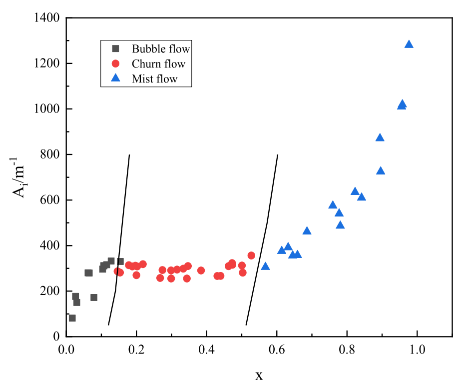

FIGURE 10. The curve of interfacial area concentration - vapor quality.

By comparing figures 7−9, it can be seen that the distribution of experimental results on the existing flow pattern diagram is close to the lower right direction. This area is the blank division of the traditional flow pattern diagram, reflecting the small flow of the surface-mounted self-circulating evaporative cooling system. Meanwhile, the characteristics of the large width to height ratio of the liquid box rectangular channel determine the transition of flow pattern from bubbly flow to churn flow. These fully demonstrated that the existing three flow pattern diagrams are not suitable for the flow pattern division of the surface-mounted evaporative cooling system.

Therefore, a prediction model of flow pattern transition in the liquid box is established based on flow heat transfer characteristics in the surface-mounted evaporative cooling system shown in Figure 10. As the outlet vapor quality of the liquid box increases, the interfacial area concentration curve shows

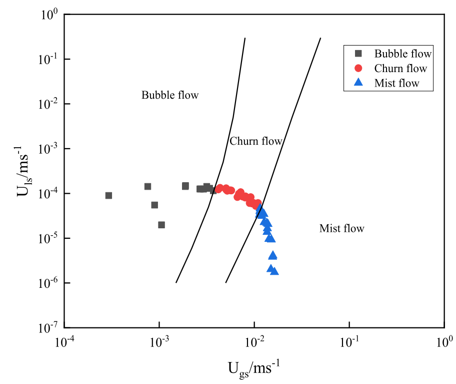

FIGURE 11. New flow pattern diagram.

a trend of increasing, stabilizing, and then gradually rising again. The two inflection points appearing in the change of the interfacial area concentration are the transition points of the flow pattern in the liquid box, which indicates that the model reflects the flow pattern in the liquid box accurately. Based on the prediction results, a flow pattern diagram with the superficial velocity as the coordinate axis is established in Figure 11. With the change of superficial velocity, the flow pattern diagram accurately reflects the evolution of the flow pattern in the liquid box, which extends to a small flow self-circulating system. This study is of great significance for the calculation of boiling heat transfer in the surface-mounted evaporative cooling system.

V. CONCLUSION

In this paper, three flow patterns in the liquid box are obtained based on the visualization experiment results. The prediction model of flow pattern is established based on the change of interfacial area concentration. The model prediction results are in good agreement with the experimental data. This provides a theoretical basis for calculating the boiling heat transfer of the surface-mounted evaporative cooling system. The main conclusions are as follows:

With the increase of thermal load, three flow patterns of bubble flow, saturated bubble flow, and mist flow appear in order in the liquid box. Due to the narrow rectangular characteristics of the liquid box and rib disturbance, small bubbles are restricted to merge into larger bubbles. Besides, the self-circulating characteristics of the system cause the pattern transition from churn flow to mist flow.

According to the experimental results, a flow pattern transition model suitable for the surface-mounted evaporative cooling system is established. The model uses the interfacial area concentration change in the liquid box as the flow pattern transition criterion, which is in good agreement with the experimental data.

REFERENCES

[1] I. Mudawar, "Assessment of high-heat-flux thermal management schemes," in *Proc. 7th Intersoc. Conf. Thermal Thermomech. Phenomena Electron. Syst.*, Jun. 2000, pp. 122–141.

[2] L. Ruan and Z. G. Li, "The discussion of energy conservation of data center from the evaporative cooling technology of HPC," in *Proc. Int. Conf. Parallel Distrib. Process. Techn. Appl. (PDPTA)*, 2012, pp. 1–5.

[3] L. Ruan and G. B. Gu, "Feasibility of evaporative cooling technology for ultra-large capacity hydraulic turbines: Selection and selection of rectangular hollow conductors in stator windings," *J. Harbin Inst. Technol.*, vol. 3, pp. 401–404, Dec. 2005.

[4] R. Cao and L. Ruan, "Feasibility study of evaporative cooling technology on converter valve," *Power Electron.*, vol. 52, no. 06, pp. 40–42, 2018.

[5] Y. T. Shi, R. Cao, and L. Ruan, "Experimental study on boiling heat transfer and flow of surface-mounted internal rib array self-circulating evaporative cooling system," *Proc. CSEE*, vol. 40, no. 06, pp. 1997–2006, 2020.

[6] P. Rollmann and K. Spindler, "A new flow pattern map for flow boiling in microfin tubes," *Int. J. Multiphase Flow*, vol. 72, pp. 181–187, Jun. 2015.

[7] G. F. Hewitt and D. Roberts, "Studies of two-phase flow patterns by simultaneous X-ray and flast photography," *Atomic Energy Res. Establishment*, vol. 1, no. 1, pp. 1–31, Feb. 1969.

[8] O. Baker, "Design of pipe lines for simultaneous flow of oil and gas," *Oil Gas J.*, vol. 53, p. 323-G, Jan. 1953.

[9] Y. Taitel and A. E. Dukler, "A model for predicting flow regime transitions in horizontal and near horizontal gas-liquid flow," *AIChE J.*, vol. 22, no. 1, pp. 47–55, Jan. 1976.

[10] T. L. Gould, M. R. Tek, and D. L. Katz, "Two-phase flow through vertical, inclined, or curved pipe," *J. Petroleum Technol.*, vol. 26, no. 8, pp. 915–926, Aug. 1974.

[11] D. B. R. Kenning and Y. Yan, "Saturated flow boiling of water in a narrow channel: Experimental investigation of local phenomena," *Chem. Eng. Res. Des.*, vol. 79, no. 4, pp. 425–436, May 2001.

[12] C. H. Guo, "Transition criteria for two-phase flow patterns in evaporative cooled turbo generators," *Chin. J. Elect. Eng.*, vol. 27, no. 17, pp. 67–71, 2007.

[13] Y. Zhu, X. Wu, and R. Zhao, "R32 flow boiling in horizontal mini channels: Part I. two-phase flow patterns," *Int. J. Heat Mass Transf.*, vol. 115, pp. 1223–1232, Dec. 2017.

[14] C. R. Kharangate, L. E. O'Neill, and I. Mudawar, "Effects of two-phase inlet quality, mass velocity, flow orientation, and heating perimeter on flow boiling in a rectangular channel: Part 1 – two-phase flow and heat transfer results," *Int. J. Heat Mass Transf.*, vol. 103, pp. 1261–1279, Dec. 2016.

[15] A. Mosyak, Z. Segal, E. Pogrebnyak, and E. Hetsroni, "Two-phase flow patterns and heat transfer in parallel microchannels," *J. Thermal Sci.*, vol. 11, no. 4, pp. 353–358, 2002.

[16] V. P. Carey and G. D. Mandrusiak, "Annular film-flow boiling of liquids in a partially heated, vertical channel with offset strip fins," *Int. J. Heat Mass Transf.*, vol. 29, no. 6, pp. 927–939, Jun. 1986.

[17] L. P. M. Colombo, A. Lucchini, and A. Muzzio, "Flow patterns, heat transfer and pressure drop for evaporation and condensation of R134A in microfin tubes," *Int. J. Refrig.*, vol. 35, no. 8, pp. 2150–2165, Dec. 2012.

[18] C.-M. Yang and P. Hrnjak, "A new flow pattern map for flow boiling of R410A in horizontal micro-fin tubes considering the effect of the helix angle," *Int. J. Refrig.*, vol. 109, pp. 154–160, Jan. 2020.

[19] Y. Taitel, D. Bornea, and A. E. Dukler, "Modelling flow pattern transitions for steady upward gas-liquid flow in vertical tubes," *AIChE J.*, vol. 26, no. 3, pp. 345–354, May 1980.

[20] M. Ishii and K. Mishima, "Two-fluid model and hydrodynamic constitutive relations," *Nucl. Eng. Des.*, vol. 82, nos. 2–3, pp. 107–126, 1984.

[21] M. Kaichiro and M. Ishii, "Flow regime transition criteria for upward two-phase flow in vertical tubes," *Int. J. Heat Mass Transf.*, vol. 27, no. 5, pp. 723–737, May 1984.

[22] L. Chen, "Flow patterns in upward two-phase flow in small diameter tubes," Ph.D. dissertation, Brunel Univ., Uxbridge, U.K., 2006.

[23] Z. Lu and X. Zhang, "Identification of flow patterns of two-phase flow by mathematical modelling," *Nucl. Eng. Des.*, vol. 149, nos. 1–3, pp. 111–116, Sep. 1994.

[24] Z. Miropolskii, P. Snelobe, and A. Kalamesebe, "Void Fraction of water-steam mixture flow with or without heat transfer," *Teploenergetika, 1971.*, vol. 5, pp. 374–379.

YITAO SHI is currently pursuing the Ph.D. degree with the University of Chinese Academy of Sciences. His major research interest includes evaporative cooling technology for electronic equipment.

RUI CAO received the master's degree from Beijing Jiaotong University, Beijing, China, in 2010. She joined the Institute of Electrical Engineering, Chinese Academy of Sciences, where she is currently a Research Assistant. Her research interest includes the heat dissipation of electronic equipment.

LIN RUAN received the Ph.D. degree in electric machines and electric apparatus from the Institute of Electrical Engineering, Chinese Academy of Sciences, Beijing, China, in 2004. She joined the Institute of Electrical Engineering, Chinese Academy of Sciences, where she is currently a Researcher. Her research interests include evaporative cooling technology for electrical and electronic equipment and two-phase flow and phase-change thermal technology.